LASERS AND AMPLIFIERS

PACS numbers: 42.60.Jf; 42.65.Yj; 42.65.Re
DOI: 10.1070/QE2009v039n05ABEH013930

Interaction of frequency-modulated light beams in multistage parametric amplifiers at the maximum gain bandwidth

S.N. Vlasov, E.V. Koposova, G.I. Freidman

***Abstract*. Conditions of the applicability of equations in the quasi-static approximation for studying the parametric interaction of frequency-modulated light beams in multistage amplifiers are considered. This approximation is used to simulate numerically processes in a multistage DKDP crystal amplifier with the output power exceeding 10 PW and suppressed luminescence.**

Keywords: *frequency modulation, light beams, parametric amplification, petawatt amplifiers, femtosecond pulses.*

1. Introduction

The possibility of optical parametric chirped pulse amplification (OPCPA) was discussed and studied as early as 1980s – 1990s [1 – 6]. By pumping BBO crystals by 100-fs, 400-nm second-harmonic pulses from a Ti : sapphire laser, the amplification of frequency-modulated radiation with the spectral width of up to ~ 1.2 fs^{-1} appearing upon self-focusing of the incident radiation was realised [3 – 7]. The amplification of such broadband radiation occurs at a certain angle between its beam and the pump beam (in the case of vector phase matching and noncollinear interaction) when the superbroadband phase-matching conditions are fulfilled at the vicinity of the central wavelength $\lambda_1^{(0)} =$ 600 nm. In this case, the difference of the effective group velocities of the signal and idler waves and the sum of coefficients of their quadratic dispersion are close to zero. After the compression of amplified radiation, pulses of duration down to 4 fs and energy of a few microjoules were obtained. Below, we will denote interacting waves by the subscript j: $j = 1$ corresponding to the signal wave, $j = 2$ – to the idler wave, and $j = 3$ or $j = \mathrm{p}$ – to the pump wave.

The superbroadband phase matching in BBO crystals was used in the last years for the development of multistage amplifiers of 5 – 10-fs pulses stretched approximately to 30 ps [8 – 17] and 1 ns [18]. As a result, 5 – 20-fs pulses of energy from ~ 1 to ~ 100 mJ and power from 0.1 to 10 TW were obtained. Pumping was performed by the 400-nm second harmonic of a Ti : sapphire laser or by second harmonics from Nd^{3+}-doped crystal lasers at 530 – 560 nm.

The possibility of using multistage parametric amplifiers of frequency-modulated light pulses to achieve petawatt powers was analysed in papers [20 – 22]. It was proposed to stretch pulses being amplified approximately up to 1 ns and to use nonlinear KDP crystals of diameter up to 20 – 30 cm in the last stage. The authors of [21] proposed to use the 438-nm third harmonic of an Asterix IV laser for pumping. In this case, the superbroadband phase-matching conditions are fulfilled in a KDP crystal for 785-nm femtosecond pulses of a Ti : sapphire laser. However, this phase matching is absent for the 530-nm pump wavelength, which is promising for the development of high-power amplifiers, and the maximum gain bandwidth is achieved in the nearly degenerate interaction regime [20, 23, 24]. This complicates the generation of high-power pulses shorter than 40 fs with the help of amplifiers based on nonlinear KDP crystals [24]. In a system based on a KDP crystal, 84-fs, 35-J pulses were obtained [24].

It was shown in [25, 26] that upon pumping at $\lambda_{\mathrm{p}}^{(0)} \approx$ 527 nm, amplifiers based on nonlinear DKDP crystals have the superbroad phase-matching band at $\lambda_1^{(0)} \approx 910$ nm. An amplifier based on this crystal with the stretcher – compressor transmission bandwidth $\Omega_{\mathrm{str}} \approx 0.1$ fs^{-1} produces 40-fs, 38-J pulses [27 – 29]. The manufacturing of the final amplification stage with the pump pulse energy of ~ 1000 J is planned. According to estimates, this will make it possible to obtain pulses of power up to a few petawatts. Such pulse durations and powers for amplifiers with nonlinear DKDP crystals are not limiting.

In this paper, we analyse the possibility of achieving the pulse power up to 10 – 20 PW by expanding the transmission band of the stretcher and compressor up to the limiting width of the superbroad gain band. The project of manufacturing amplifiers based on DKDP crystals pumped by 1 – 10-ps pulses with a high repetition rate and peak powers up to a few petawatts is discussed in [30]. Such amplifiers also should have the gain bandwidth close to the limiting spectral width of a signal being amplified.

An important question appearing in the development of high-power amplifiers is the question about the intensity decrease rate in the focal spot at the leading edge of a pulse after focusing of compressed radiation. The radiation intensity before the main pulse at the interval exceeding 30 – 40 ps is determined by spontaneous luminescence. This interval for OPCPA systems is determined by the pump pulse duration, and contrast in this interval can be considerably higher than that for laser CPA systems because

S.N. Vlasov, E.V. Koposova, G.I. Freidman Institute of Applied Physics, Russian Academy of Sciences, ul. Ul'yanova 46, 603950 Nizhnii Novgorod, Russia; e-mail: vlasov@hydro.appl.sci-nnov.ru, ev_kopos@mts-nn.ru, gif@appl.sci-nnov.ru

Received 17 June 2008
Kvantovaya Elektronika **39** (5) 393 – 404 (2009)
Translated by M.N. Sapozhnikov

parametric luminescence is not isotropic but is concentrated near the phase-matching cone. If the phase-matching cone of a subsequent channel is inverted with respect to the luminescence cone of a previous channel (or vice versa), parametric luminescence is concentrated within a narrow region along the tangential plane of these cones [31, 32]. In systems with such preliminary amplification stages, the relative level of parametric luminescence not exceeding 10^{-8} was achieved for pulse powers $\sim 1-10$ TW [14, 18]. In laser CPA systems without the additional suppression of luminescence, contrast is two-three orders of magnitude lower [33, 34]. However, when compressed radiation is focused, the difference between laser CPA systems and OPCPA systems is determined only by the lifetime of spontaneous luminescence.

In multistage parametric amplifiers with the output power $\sim 1-10$ PW, as in laser CPA systems with the high total gain $G_{\rm m} \approx 10^{11}-10^{12}$, the number $N_{\rm d}$ of spontaneous luminescence photons propagated for the time $2T_{\rm p}$ through the focal spot of radiation with the diffraction divergence is proportional to the product of $G_{\rm m}$ by the number of amplified longitudinal modes (i.e. to the product of the gain bandwidth $\Delta\Omega$ by the pump pulse duration): $N_{\rm d} \approx \Delta\Omega T_{\rm p} G_{\rm m}$. The spontaneous emission intensity $I_{\rm sd}$ in this region and the emission power density $w_{\rm sd}$ propagated through the focal spot of area $a_{\rm d}^2 \approx 10^{-6}-10^{-7}$ cm^2 achieve rather high values of $10^{12}-10^{13}$ W cm^{-2} and 10^3-10^4 J cm^{-2}, respectively, for $T_{\rm p} \sim 1$ ns.

The values of $I_{\rm sd}$ and $w_{\rm sd}$ can be reduced by the methods similar to those developed for laser CPA systems [19, 33–35]. In [19], a parametric amplifier pumped by 4-ps pulses was used to generate 300-fs, 100-μJ pulses, which were then amplified in a CPA amplifier. In [33–35], similar pulses were generated by using the preliminary amplification (or amplification with recompression) of the initial femtosecond pulse, its subsequent 'purification' from noise emission and stretching in a stretcher. The properties of processes in the simplest OPCPA system, similar to those considered above, are analysed in section 3 of this paper.

30–40 ps before the pulse maximum the contrast begins to deteriorate rapidly and achieves $\sim 10^{-6}$ approximately 10 ps before the pulse maximum [18, 34]. The contrast in this region is mainly determined by the defects of diffraction gratings of the stretcher and compressor with the depth $h \leqslant 0.1\lambda_1^{(0)}$ and the characteristic transverse size $\varDelta_r \sim 1$ mm [34]. The focusing of a compressed radiation beam of diameter $D_{\rm c} \sim 10$ cm reduces the influence of defects of compressor gratings by approximately $(\varDelta_r/D_{\rm c})^2 \approx 10^4$ times. The influence of defects of stretcher gratings is reduced less considerably, but its reduction will be noticeable ($10^{-2}-10^{-3}$) if the beam diameter $D_{\rm str}$ is large enough ($\sim 1-3$ cm). Therefore, the shape of the leading edge of a pulse in the focal plane down to the level $10^{-8}-10^{-10}$ of the peak intensity will be determined by coherent processes in the amplifier stages and the stretcher–compressor system. We analyse in section 3 with this accuracy the factors determining the shape and steepness of the leading edge of a pulse and the pulse contrast in the interval up to a few picoseconds from its maximum.

To analyse the processes of parametric amplification of frequency-modulated radiation beams in the field of a transform-limited pump pulse, the authors of [25] proposed to use equations for the amplitudes of interacting waves in quasi-stationary and quasi-static approximations, which take into account the dependence of the shift of wave packets on the local frequency due to their different directions and different group velocities, and also the dependence of the wave detuning on the local frequency. In section 2, we analyse the possibility of application of similar equations for studying the parametric amplification of frequency-modulated radiation beams in the field of 'short' 1–10-ps frequency-modulated 'inclined' pump wave packets. We also considered the question about the maximum length of nonlinear elements of amplifiers pumped by pulses of duration close to the minimal and with the limiting gain bandwidth. Based on equations in the quasi-static approximation, we performed in section 3 the numerical simulation of processes for several variants of multistage parametric DKDP crystal amplifiers. Aside from the questions mentioned above, this also allowed us to elucidate some general properties of parametric amplification in multistage systems.

2. Quasi-stationary and quasi-static light beams

In the case of the optimally selected parameters of parametric amplifiers of femtosecond pulses of duration $2\tau_0$ stretched in a stretcher up to $2T_1 \gg 2\tau_0$, the relative shift of the interacting wave packets and the change in their duration during propagation in a nonlinear element should be smaller than T_1: $d|\Delta K'_{\max}| < T_1$, where d is the element length; $\Delta K'_{\max}$ is the maximum difference of the moduli of wave vectors $S_j = K'_j(\omega_j)$ of the interacting waves; and K_j is the wave number. Hereafter, the prime denotes the derivative with respect to frequency. We assume that the pulse has a Gaussian shape. In addition, when the choice of these parameters is reasonable, the interaction of the waves will lead to slow variations in their amplitudes and phases. Therefore, it is reasonable to analyse parametric interaction in such amplifiers in a weakly linear approximation, in which wave eikonals satisfy linear dispersion relations.

In broadband multistage amplifiers, the type I (e–oo) interaction is used. We shall restrict our consideration to this interaction. We assume that the signal wave with spectral components propagating in one direction (collimated beam) is incident on a nonlinear element long the normal to its surface parallel to the z axis. After propagation through a stretcher, the phase of spectral amplitudes of this radiation changes by the value of $\varPhi_{\rm str}^{(0)}$ depending on the shift Ω_1 of the carrier frequency ω_1 from its central value $\omega_1^{(0)}$ $(\omega_1 = \omega_1^{(0)} + \Omega_1)$. It is known the pulse shape is determined only by the nonlinear component of this dependence: $\varPhi_{\rm str}(\Omega_1) = \varPhi_{\rm str}^{(0)}(\Omega_1) - \varPhi_{\rm str}'^{(0)}(0)\Omega_1$. It can be shown by the stationary phase method that the signal wave amplitude behind the stretcher is proportional to the spectral amplitude $A_1^{(0)}(\boldsymbol{r}_\perp, \Omega_1)$ of the initial pulse, while the variable frequency $\Omega_1(t)$ is defined in the implicit form

$$
\begin{aligned}
A_1(\boldsymbol{r}_\perp, t) &= \left(\frac{\mathrm{i}}{2\pi|\varPhi''_{\rm str}(\Omega_1(t))|}\right)^{1/2} A_1^{(0)}(\boldsymbol{r}_\perp, \Omega_1(t)) \\
&\times \exp[-\mathrm{i}\varPhi_1^{(0)}(t)], \qquad t = \frac{\mathrm{d}\varPhi_{\rm str}(\Omega_1(t))}{\mathrm{d}\Omega_1}, \\
\varPhi_1^{(0)}(t) &= \int_0^t \Omega_1(t)\mathrm{d}t = \varPhi_{\rm str}(\Omega_1(t)) + t\Omega_1(t),
\end{aligned} \tag{1}
$$

the local frequency $\Omega_1(t)$ changes with time almost linearly as $\Omega_1(t) \approx \dot{\Omega}_1 t$, $\dot{\Omega}_1 = \Omega_0/T_1$. The quantity $\Omega_0 = 1/\tau_0$ is the spectral half-width of a femtoseconds pulse, and the pulse stretching coefficient $K_{\rm str} = \Phi''_{\rm str}\Omega_0^2 \geqslant 1$ determines the pulse duration $T_1 = \tau_0 K_{\rm str}$ after its propagation through the stretcher. The stretcher is characterised by the transmission bandwidth $\Omega_{\rm str}$ and the wave train duration $T_{\rm str} = |\Phi''_{\rm str}|\Omega_{\rm str}$. These parameters are usually selected to provide conditions $\Omega_{\rm str} \geqslant 4\Omega_0$ and $T_{\rm str} \geqslant 4T_1$.

Pump radiation with the pulse duration $2T_{\rm p} \geqslant T_{\rm str}$ is also frequency-modulated in the general case: $\omega_{\rm p} = \omega_{\rm p}^{(0)} + \Omega_{\rm p}(t)$, where $\Omega_{\rm p}(t) \approx \Omega_{\rm p}^{(0)}(t/T_{\rm p})$; $\Omega_{\rm p}^{(0)} = 1/\tau_{\rm p}^{(0)}$; and $2\tau_{\rm p}^{(0)}$ is the duration of the initial transform-limited pulse. Pump radiation is incident on a nonlinear element at an angle of $\Psi_{\rm p}$ to the z axis in the zx plane, to which the optical axis of the nonlinear crystal is parallel [for definiteness, we assume that the axis of this beam (the z_3 axis) is inclined in the direction of negative values of x]. In some cases, the wave packet of pump radiation should be made 'inclined'. Such a wave packet is obtained when a collimated wave packet propagates through a refracting (or reflecting) dispersion element, for example, a prism (or is reflected from a diffraction grating). The width of the pump spectrum is usually considerably smaller than the carrier frequency: $\Omega_{\rm p}^{(0)}/\omega_{\rm p}^{(0)} \ll 1$. Therefore, the complex amplitudes $A_{\rm p}$ of the 'inclined' pump wave packet at the boundary of a nonlinear element can be written in the geometrical optics approximation in the form

$$A_{\rm p}(\boldsymbol{r}_\perp, t) = A_{\rm p}^{(0)}\big(\tilde{\boldsymbol{r}}_\perp, \Omega_{\rm p}(t_{\rm p}^{(x)})\big) \exp\left[-{\rm i}\int_0^{t_{\rm p}^{(x)}} \Omega_{\rm p}(t_1){\rm d}t_1\right],$$

$$t_{\rm p}^{(x)} = t + S_{\rm p}^{(x)}x, \qquad (2)$$

$$A_{\rm p}^{(0)}\big(\tilde{\boldsymbol{r}}_\perp, \Omega_{\rm p}(t_{\rm p}^{(x)})\big) = f_{\rm p}\left(\frac{\tilde{x}}{a_{\rm p}}, \frac{y}{a_{\rm p}}\right) A^{(0)}\left(\frac{t_{\rm p}^{(x)}}{T_{\rm p}}\right)$$

$$\times \exp\left\{-{\rm i}xq_0\left[\frac{\Omega_{\rm p}(t_{\rm p}^{(x)})}{\omega_{\rm p}^{(0)}}\right]^2\right\}.$$

Here,

$$S_{\rm p}^{(x)} = \frac{\cos\Psi_{\rm p}}{c}(\tan\theta_{\rm t} + \tan\Psi_{\rm p});$$

$$\tilde{x} = \left[x\cos\Psi_{\rm p}^{(0)} + \Delta z\tan\theta_{\rm t}\frac{\Omega_{\rm p}(t_{\rm p}^{(x)})}{\omega_{\rm p}^{(0)}}\right];$$

$q_0 = k_{\rm p}^{(0)}m_1\tan\theta_{\rm t}$; $k_{\rm p}^{(0)} = \omega_{\rm p}^{(0)}/c$; $m_1 \simeq 1$; Δz is the distance from the intersection point of central beams; $f_{\rm p}(0,0) = 1$; $a_{\rm p}$ is the pump beam diameter; and $\theta_{\rm t}$ is the wave-front tilt angle with respect to the pump beam axis. The angle $\theta_{\rm t}$ for a prism in the case of normal incidence is determined by its refraction angle $\Psi_{\rm pr}$ and the first-order dispersion $n_{\rm pg} = cK'_{\rm pr}$:

$$\tan\theta_{\rm t} = \tan\Psi_{\rm pr}\frac{n_{\rm pg} - n_{\rm pr}}{n_{\rm pr}},$$

where $n_{\rm pr}$ is the refractive index of the prism; in this case,

$$m_1 = \cos\Psi_{\rm p}\left\{1 + \frac{1}{2}\left[\tan\theta_{\rm t}(\tan\Psi_{\rm pr} + \tan\Psi_{\rm p}) + \frac{\omega_{\rm p}^{(0)}n''_{\rm pr}}{n'_{\rm pr}}\right]\right\}.$$

It is assumed that the transverse structure of the beam at the input to the dispersion element is independent of time.

The idler wave at frequency $\omega_2 = \omega_3 - \omega_1$ is excited in the nonlinear element of the amplifier. Therefore, the transverse component of its wave vector is equal to the transverse component of the pump wave vector, and its phase at the boundary $(z = 0)$ is equal to the phase difference of the pump and signal waves:

$$\Phi_2^{(0)}(x,\tau) = \Phi_{\rm p}^{(0)}(x,\tau) - \Phi_1^{(0)}(x,\tau)$$

$$= -\int_0^t \Omega_1^{(0)}(t_1){\rm d}t_1 + \int_0^{t+S_{\rm p}^{(x)}x} \Omega_{\rm p}^{(0)}(t_1){\rm d}t_1.$$

Here, we introduced a new variable – the 'local' time $\tau = t - zS_0$, where $S_0 = 1/v_0$ and v_0 is the group velocity of some of the waves at the central frequency (we assume below that $v_0 = v_1^{(0)}$ is the group velocity of the signal wave).

Based on the considerations presented above, the fields $\boldsymbol{E}_j$ of the waves interacting in the nonlinear element of the amplifier can be written in the form

$$\boldsymbol{E}_j = \frac{\boldsymbol{e}_j}{2}\left(\frac{\lambda_j^{(0)}I_{\rm p}}{\lambda_{\rm p}^{(0)}n_j^{(0)}}\right)^{1/2} A_j(\boldsymbol{r}_\perp, z, \tau)\exp\big\{-{\rm i}\big[\big(k_{jx}x - k_{jz}z$$

$$+ \omega_j^{(0)}t\big) + \Phi_j(x,z,\tau)\big]\big\} + {\rm c.c.}, \qquad (3)$$

where $n_j^{(0)}$ is the refractive index of the medium, and the wave amplitudes A_j are normalised so that the square of their modulus is proportional to the photon flux density at the central frequency of the corresponding wave divided by the photon flux density of the pump wave with the specified intensity $I_{\rm p}$. Functions $\Phi_j(x,z,\tau)$, which we will call the eikonals of the corresponding waves, are defined by linear dispersion equations

$$\Delta K_{jz}\big(p_j^{(t)}, p_j^{(x)}\big) + p_j^{(x)} = 0,$$

$$p_j^{(t)} = \frac{\partial\Phi_j}{\partial\tau}, \quad p_j^{(x)} = \frac{\partial\Phi_j}{\partial x}, \quad p_j^{(z)} = \frac{\partial\Phi_j}{\partial z}. \qquad (4)$$

The quantities $\Delta K_{jz}(p_j^{(t)}, p_j^{(x)})$ are defined by expressions

$$\Delta K_{jz}\big(p_j^{(t)}, p_j^{(x)}\big) = \big[K_{jz}\big(\omega_j, p_j^{(x)}\big) - k_{jz} - S_0 p_j^{(t)}\big],$$

$$k_{jz} = K_{jz}\big(\omega_j^{(0)}, 0\big), \quad \omega_j = \omega_j^{(0)} + p_j^{(t)}.$$

Here, we have

$$K_{jz}\big(\omega_j, p_j^{(x)}\big) = \big[K_j^2 - (k_{jx} + p_j^{(x)})^2\big]^{1/2},$$

$$K_j = \frac{\omega_j}{c}[\varepsilon_{\rm o}(\omega_j)]1/2, \quad k_{1x} = 0, \quad k_{2x} = k_{{\rm p}x} = k_{\rm p}^{(0)}\sin\Psi_{\rm p}$$

for ordinary signal and idler waves $(j = 1, 2)$ and

$$K_{{\rm p}z}\big(\omega_{\rm p}, p_{\rm p}^{(x)}\big) = -\beta_{\rm p}\big(k_{{\rm p}x} + p_{\rm p}^{(x)}\big)$$

$$+ \big[K_{\rm e}^2(\theta_{\rm p}, \omega_{\rm p}) - \big(k_{{\rm p}x} + p_{\rm p}^{(x)}\big)^2(1 + \delta\varepsilon_{\rm oe} - \beta_{\rm p}^2)\big]^{1/2}$$

for the pump wave, where

$$K_{\rm e}^2(\theta_{\rm p}, \omega_{\rm p}) = \frac{\omega_{\rm p}^2}{c^2}\frac{\varepsilon_{\rm o}(\omega_{\rm p})\varepsilon_{\rm e}(\omega_{\rm p})}{\varepsilon_{\rm e}(\omega_{\rm p})\cos^2\theta_{\rm p} + \varepsilon_{\rm o}(\omega_{\rm p})\sin^2\theta_{\rm p}};$$

$$K_{\rm p} = \left[K_{\rm e}^2(\theta_{\rm p},\omega_{\rm p}) - k_{{\rm p}x}^2\left(1+\delta\varepsilon_{\rm oe}-\beta_{\rm p}^2\right)\right]^{1/2};$$

$$\delta\varepsilon_{\rm oe} = \beta_{\rm p}\cot(2\theta_{\rm p});$$

$$\beta_{\rm p} = \frac{[\varepsilon_{\rm o}(\omega_{\rm p}) - \varepsilon_{\rm e}(\omega_{\rm p})]\sin(2\theta_{\rm p})}{2[\varepsilon_{\rm e}(\omega_{\rm p})\cos^2\theta_{\rm p} + \varepsilon_{\rm o}(\omega_{\rm p})\sin^2\theta_{\rm p}]}$$

is the birefringence angle; the subscripts 'e' and 'o' correspond to the extraordinary and ordinary waves, respectively; and $\theta_{\rm p}$ is the angle between the z axis and the optical axis of the crystal.

We will write the solution of equations (4) in the geometrical optics approximation (assuming that $p_j^{(x)2} = 0$) and neglect the dispersion of birefringence:

$$\begin{aligned}
\Phi_j(x,z,\tau) &= \Phi_j^{(0)}\left(x_j^{(0)}, t_j^{(0)}\right) \\
&\quad - z\left[\Delta K_{jz}\left(p_j^{(t0)}\right) - p_j^{(t0)}\tilde{S}_j - p_j^{(x0)}\tilde{\beta}_j\right], \\
\Phi_1^{(0)}\left(t_1^{(0)}\right) &= \int_0^{t_1^{(0)}} \Omega_1^{(0)}(t_1)\mathrm{d}t_1, \\
\Phi_{\rm p}^{(0)}(x,\tau) &= \int_0^{t_{\rm p}^{(0)}+S_{\rm p}^{(x)}x_{\rm p}^{(0)}} \Omega_{\rm p}^{(0)}(t_1)\mathrm{d}t_1, \\
\Phi_2^{(0)}(x,\tau) &= \left[-\int_0^{t_2^{(0)}} \Omega_1^{(0)}(t_1)\mathrm{d}t_1 \right. \\
&\quad \left. + \int_0^{t_2^{(0)}+S_{\rm p}^{(x)}x_2^{(0)}} \Omega_{\rm p}^{(0)}(t_1)\mathrm{d}t_1\right], \qquad (5) \\
p_1^{(t0)} &= \Omega_1\left(t_1^{(0)}\right), \quad p_1^{(x0)} = 0, \quad p_{\rm p}^{(t0)} = \Omega_{\rm p}\left(t_{\rm p}^{(0)} + S_{\rm p}^{(x)}x_{\rm p}^{(0)}\right), \\
p_{\rm p}^{(x0)} &= S_{\rm p}^{(x)}\Omega_{\rm p}\left(t_{\rm p}^{(0)} + S_{\rm p}^{(x)}x_{\rm p}^{(0)}\right), \\
p_2^{(t0)} &= -\Omega_2\left(t_2^{(0)}\right) + \Omega_{\rm p}\left(t_2^{(0)} + S_{\rm p}^{(x)}x_2^{(0)}\right), \\
p_2^{(x0)} &= S_{\rm p}^{(x)}\Omega_{\rm p}\left(t_2^{(0)} + S_{\rm p}^{(x)}x_2^{(0)}\right), \\
t_j^{(0)} &= \tau - z\tilde{S}_j\left(p_j^{(t0)}, p_j^{(x0)}\right), \quad x_j^{(0)} = x - \tilde{\beta}_j z,
\end{aligned}$$

where

$$\tilde{S}_j\left(p_j^{(t0)}, p_j^{(x0)}\right) = \left\{K'_{jz}(\omega_j,0)\left[1 + \frac{k_{jx}p_j^{(x0)}}{K_{jz}^2(\omega_j,0)}\right] - S_0\right\};$$

$$\tilde{\beta}_2 = -\frac{k_{{\rm p}x}}{K_{2z}(\omega_j,0)}; \quad \tilde{\beta}_{\rm p} = -\left[\beta_{\rm p} + \frac{k_{{\rm p}x}\left(1+\delta\varepsilon_{\rm oe}-\beta_{\rm p}^2\right)}{K_{\rm p}}\right].$$

Equations for the amplitudes $A_j(\boldsymbol{r}_\perp, z, \tau)$ of the interacting waves are similar to usual equations of quasi-optics describing three-wave interactions with parameters depending on local frequencies $\omega_j = \omega_j^{(0)} + p_j^{(t0)}$ and transverse components $-p_j^{(x0)}$ of waves vectors. In the general case, a linear operator $\hat{R}_j$ should be added to the left-hand side of these equations, which takes into account the influence of the finite rate of frequency changing on the change of amplitudes, as well as the second- and third-order dispersion:

$$\begin{aligned}
&\frac{\partial A_1}{\partial z} + \tilde{S}_1(\omega_1)\frac{\partial A_1}{\partial \tau} + \frac{\mathrm{i}}{2K_1}\Delta_\perp A_1 + \hat{R}_1 A_1 \\
&\quad = \mathrm{i}\gamma_1(\omega_1)A_{\rm p}A_2^*\exp[\mathrm{i}\Delta\Phi(x,z,\tau)], \\
&\frac{\partial A_2}{\partial z} + \tilde{\beta}_2(\omega_2)\frac{\partial A_2}{\partial x} + \tilde{S}_2(\omega_2)\frac{\partial A_2}{\partial \tau} + \frac{\mathrm{i}}{2K_{2z}}\Delta_\perp A_2 + \hat{R}_2 A_2 \\
&\quad = \mathrm{i}\gamma_2(\omega_2)A_{\rm p}A_1^*\exp[\mathrm{i}\Delta\Phi(x,z,\tau)], \qquad (6) \\
&\frac{\partial A_{\rm p}}{\partial z} + \tilde{\beta}_{\rm p}\frac{\partial A_{\rm p}}{\partial x} + \tilde{S}_{\rm p}(\omega_{\rm p})\frac{\partial A_2}{\partial \tau} + \frac{\mathrm{i}}{2K_{{\rm p}z}}\Delta_\perp A_{\rm p} + \hat{R}_{\rm p} A_{\rm p} \\
&\quad = \mathrm{i}\gamma_{\rm p}(\omega_{\rm p})A_1A_2\exp[-\mathrm{i}\Delta\Phi(x,z,\tau)], \\
&\hat{R}_j = -\frac{K''_{{\rm p}z}\dot{\Omega}_j}{2} - \mathrm{i}\,\frac{K''_{{\rm p}z}}{2}\frac{\partial^2}{\partial\tau^2} - \frac{K'''_{{\rm p}z}}{6}\frac{\partial^3}{\partial\tau^3}.
\end{aligned}$$

Here, $\dot{\Omega}_j = \partial\Omega_j/\partial\tau$. The interaction coefficients $\gamma_j(\omega_j) = \gamma_0 f_j(\omega_j)$ of the waves are determined by expressions

$$\gamma_0 = \chi\sqrt{I_{\rm p}},$$

$$f_j(\omega_i) = \frac{n_j^{(0)}}{n_j\cos\tilde{\beta}_j}\left(1 + \frac{\Omega_j}{\omega_j^{(0)}}\right),$$

where

$$\chi = d_{\rm eff}\left(\frac{2\omega_1^{(0)}\omega_2^{(0)}}{\varepsilon_0 c^3 n_1^{(0)}n_2^{(0)}n_{\rm p}^{(0)}}\right)^{1/2}.$$

Here, χ is measured in $\mathrm{W}^{-1/2}$; $d_{\rm eff}$ is the effective nonlinearity of the crystal; and ε_0 is the permittivity of vacuum.

The amplification process depends most strongly on the dependence of the phase detuning $\Delta\Phi(z,x,\tau)$ on the local values of $p_j^{(t0)}$ and $-p_j^{(x0)}$:

$$\Delta\Phi(x,z,\tau) = [\Phi_1(x,z,\tau) + \Phi_2(x,z,\tau) - \Phi_3(x,z,\tau)].$$

Small variations in the refractive index caused by cubic nonlinearity in right-hand sides of equations (6) can be taken into account in the obvious way. We assumed in calculations that the anisotropy and dispersion of this nonlinearity are small, so that the nonlinear refractive index Δn_j for the jth wave can be described by expressions for an isotropic medium [36]

$$\begin{aligned}
\Delta n_j &= \frac{1}{2}n_2\left(|E_j|^2 + 2|E_l|^2 + \frac{2}{3}|E_{\rm p}|^2\right) \quad (j=1,2,\ l=1,2), \\
\Delta n_{\rm p} &= \frac{1}{2}n_2\left(\frac{2}{3}|E_1|^2 + \frac{2}{3}|E_2|^2 + |E_{\rm p}|^2\right). \qquad (7)
\end{aligned}$$

Based on the data presented in [37], we can assume that the B integral in a nonlinear DKDP crystal for pump radiation is $3.2\times10^{-2}dI_{\rm p}$, were d is the crystal length and $I_{\rm p}$ is measured in GW cm^{-2}. Taking this into account, the value of $\frac{1}{2}n_2$ was determined in specific calculations.

By varying the pump-beam tilt angle $\theta_{\rm t}$, we can compensate the group mismatch of the signal and pump within some limits and change the gain bandwidth (see, for example, [7, 32, 38]. However, for $S_{\rm p}^{(x)} \neq 0$, the phase of the frequency-modulated pump and, therefore, the phase mismatch $\Delta\Phi$ depend on the transverse coordinate x and time. In parametric amplifiers, where the pump spot radius $a_{\rm p}$ is of the order of the length $L_{\rm p} = cT_{\rm p}$ or exceeds it, this can lead to the chromatic dependence of the signal phase on x. In addition, in these cases, when the pump-pulse front is strongly inclined with respect to the entrance surface of the nonlinear element, the pump-pulse shape and, hence, the amplified-beam shape will be nonstationary. Therefore, the tilt angle $\theta_{\rm t}$ in parametric amplifiers of high-power short pulses should be chosen so that the front of the pump pulse would be parallel to the entrance surface of the nonlinear element ($S_{\rm p}^{(x)} = 0$). In this case, due to quadratic angular dispersion, the dependence of the propagation direction of the pump beam on the local pump frequency is weak: $\Delta\Psi_{\rm p} \approx \tan\theta_{\rm t}(\Omega_{\rm p}(t)/\omega_{\rm p}^{(0)})^2$ [see (2)]. If the nonlinear element length d is restricted by the relation

$$|\beta_{\rm p2}|q_0\left[\frac{\Omega_{\rm p}\left(t_{\rm p}^{(x)}\right)}{\omega_{\rm p}^{(0)}}\right]^2 d < \frac{\pi}{2} \quad (\beta_{\rm p2} = \tilde{\beta}_{\rm p} - \tilde{\beta}_2),$$

this dependence will affect neither the gain nor the phase of the amplified signal. We will restrict our consideration to this one-dimensional approximation for eikonals.

Relations (5) for eikonals and equations (6) for the amplitudes of frequency-modulated waves determine amplification processes in a broad interval of parameters. The amplification of sufficiently smooth pulses in parametric amplifiers operating in the nearly optimal regime can be described by replacing expressions (5) and (6) by equations considerably simplifying the numerical simulation of the operation of multistage amplifiers. This is related to the fact that the time shifts of the amplified waves with respect to each other and the pump pulse in nonlinear elements of such amplifiers should be smaller than the duration of these pulses: $|S_{j\max}|d < T_{\rm str}, T_{\rm p}$. If this condition is not fulfilled, then, as was shown already in the first study of the influence of the group-velocity dispersion of interacting waves on parametric amplification processes [39], a strong modulation of the amplitude of these pulses occurs at the nonlinear stage of interaction and, therefore, the spectrum of the amplified signal is considerably distorted. In the case of small relative shifts of the interacting pulses, the expression for the phase mismatch can be written in the form

$$\Delta\Phi(z,\tau) \approx z\Delta K(z,\tau),\ \ \Delta K(z,\tau) = [\Delta K(\tau) - \delta k(z,\tau)];$$

$$\Delta K(\tau) = [\Delta K_1(\Omega_1(\tau)) + \Delta K_{2z}(\Omega_2(\tau)) - \Delta K_{{\rm p}z}(\Omega_{\rm p}(\tau))] + \Delta k_0; \qquad (8)$$

$$\delta k(z,\tau) = z\left[\dot{\Omega}_1\,\frac{\tilde{S}_1^2(\tau) - \tilde{S}_2^2(\tau)}{2} + \dot{\Omega}_{\rm p}\,\frac{\tilde{S}_{\rm p}^2(\tau) - \tilde{S}_2^2(\tau)}{2}\right].$$

Here, $\Omega_2(\tau) = \Omega_{\rm p}(\tau) - \Omega_1(\tau)$; $\Delta k_0 = k_1 + k_{2z} - k_{{\rm p}z}$; and $\tilde{S}_j(\tau) = K'_{jz} - S_0$. The quantity $\delta k(z,\tau)$ proportional to the longitudinal coordinate characterises a change in the wave-detuning modulus $\Delta K(z,\tau)$ due to a finite rate of the frequency change (due to the frequency 'slipping' effect). The influence of this term on the amplification process increases with increasing the gain bandwidth and decreasing the duration $T_{\rm str}$ of the stretched pulse. Therefore, we consider the case of short pump pulse durations $T_{\rm p}$ ($\sim$ 1 ps) at which the pump pulse intensity $I_{\max}$ below the breakdown threshold increases up to a few tens GW cm^{-2} [because $I_{\max} \approx I_0(T_{\rm p}^{(0)}/T_{\rm p})^{1/2}$, $T_{\rm p}^{(0)} = 1$ ns]. As a result, the gain bandwidth also increases. This limiting width $\Delta\Omega_{\max}$ can be estimated from the condition $[|\Delta\tilde{K}(z,\Omega_1(\tau))| \times (2\gamma_0)^{-1}]^2 \leqslant 0.25$. When this condition is fulfilled, the wave detuning ΔK weakly affects the gain of plane waves determined in the linear quasi-static approximation:

$$G(z,\tau) = \cosh(p_0 z)^2\left\{1 + \left[\frac{\Delta\tilde{K}}{2p_0}\tanh(p_0 z)\right]^2\right\},$$

$$p_0(\tau) = \left[\gamma_0^2(\tau) - \frac{\Delta\tilde{K}^2}{4}\right]^{1/2}$$

[to simplify the expression, it is assumed that $f_j(\omega_j) = 1$]. We will assume in estimates that $I_{\max} = 25$ GW cm^{-2}.

Figures 1 and 2 present the characteristics of the superbroadband phase matching (wave detunings ΔK and projections of beam vectors $\tilde{\boldsymbol{S}}_j$) for a BBO crystal ($S_{\rm p}^{(0)} =$ 1.37 ps cm^{-1}, $\chi = 6.1$ GW$^{-1/2}$) of length up to $\sim 0.2T_{\rm str}/S_{\rm p}^{(0)}$ pumped by the second harmonic 100-fs, 400-nm pulses of a Ti:sapphire laser stretched up to $2T_{\rm p} \approx T_{\rm str} \approx 1$. The functions ΔK and $\tilde{S}_j$ are constructed based of the Sellmeyer relations presented in [40]. It follows from these data that for the length of a nonlinear element $d < 0.1T_{\rm str}/S_{\rm p}^{(0)}$, the relative frequency shift weakly affects the interaction of waves in the gain band -0.6 fs$^{-1} \leqslant \Omega_1 \leqslant 0.6$ fs^{-1}. The amplification of smooth signals in this region of parameters can be described in the quasi-static approximation: $\tilde{S}_j = 0$, $\Delta\tilde{K}(z,\Omega_1) = \Delta K(\Omega_1)$.

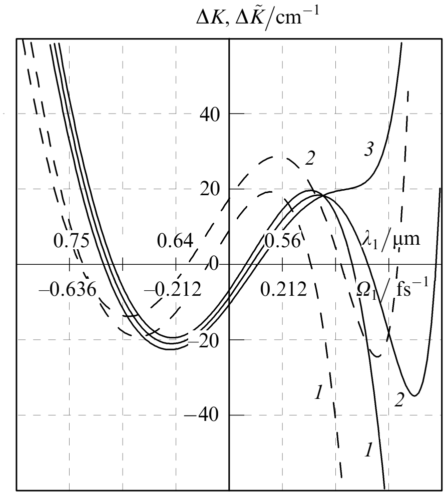

Figure 1. Dependences of the wave detunings in a BBO crystal on the shift of frequency Ω_1 and wavelength of a signal for $\lambda_3^{(0)} = 0.4$ μm: stationary detuning $\Delta K(\Omega_1)$ (*1*), $\Delta\tilde{K}(z,\Omega_1)$ for $z = 0.5d_{\rm m}$ μm (*2*) and $z = d_{\rm m}$ (*3*) for $\dot{\Omega}_3 > 0$, $\theta_3 = 27.3°$, $\Psi_{\rm p} = 5.67°$ (solid curves) and also $\Delta K(\Omega_1)$ (*1*) and $\Delta\tilde{K}(z,\Omega_1)$ for $z = d_{\rm m}$ (*2*) for $\dot{\Omega}_3 < 0$, $\theta_3 = 27.6°$, $\Psi_{\rm p} = 6.13°$ (dashed curves).

As the length d is increased up to $d_{\rm m} = 0.2T_{\rm str}/S_{\rm p}^{(0)}$, the 'wave matching' band as if broadens – in the high-frequency part of this band, where the difference of group velocities of the amplified waves rapidly increases with increasing frequency, a region appears in which the 'wave matching' is established in the second half of the nonlinear element. As d is further increased, the wave detuning at the end of the nonlinear element begins to increase at the gain band centre.

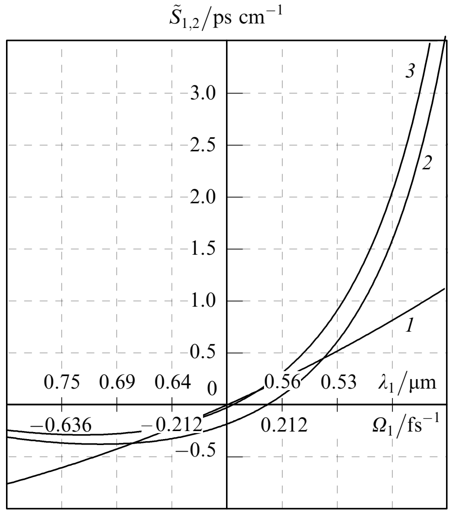

Figure 2. Dependences of the projections of beam vectors $\tilde{S}_1$ on Ω_1 and λ_1 for $\theta_3 = 27.3°$, $\Psi_p = 5.67°$ (*1*), $\tilde{S}_2$ for $\theta_3 = 27.3°$, $\Psi_p = 5.67°$ (*2*), and $\tilde{S}_2$ for $\theta_3 = 27.6°$, $\Psi_p = 6.13°$.

Thus, the maximum length of the nonlinear element during the amplification of a signal in a band with the limiting width $\Delta\Omega_{max} \approx 1.2$ fs^{-1} for $T_{str} \approx 1$ ps can be considered equal to $d_m = 0.2T_{str}/S_p^{(0)}$. The maximum gain $G_m = [\cosh(\gamma_0 d_m)]^2$ of a stage, by neglecting the relative pulling down of beams for $T_{str} \approx 1$ ps achieves 2500. A change in the sign of the frequency modulation of the pump leads to a red shift of the gain band. In this case, the frequency 'slipping' effect is manifested at a larger length of the nonlinear element (for $d_m = 0.35T_{str}/S_p^{(0)}$, see Fig. 1). To elucidate the possibility of using the effect of 'broadening of the wave matching band' at $d \approx d_m$ for increasing the spectral width of the amplified signal, it is necessary to analyse the amplification process by using the complete system of equations in the quasi-stationary approximation.

The interaction coefficient of waves in the DKDP crystal is an order of magnitude lower than that in the BBO crystal, but dispersion is also approximately an order of magnitude smaller (for example, $S_p^{(0)} = 0.235$ ps cm^{-1}). Because of this, the situation in the DKDP crystal is similar, however, the limiting gain bandwidth is somewhat smaller ($\Delta\Omega_{max} \approx 0.8$ fs^{-1}). In addition, because the interaction coefficient of waves in the DKDP crystal is an order of magnitude lower than that in the BBO crystal, the length of a nonlinear element should be chosen taking into account the requirement of a smallness of the nonlinear phase incursion caused by the cubic nonlinearity.

3. DKDP crystal amplifier with the output power above 10 PW and suppressed luminescence

To analyse the operation of the amplifier in the quasi-static approximation, we prepared a program for simulating processes in a multistage (up to five stages) amplifier. The number of a stage is denoted by the subscript n, $n = 0$ referring to waves at the system input, i.e. at the first stage input. Processes were simulated both in one-dimensional approximation and upon interaction of wave beams taking into account their transverse structure and different directions of group velocities and diffraction. In the latter case, the investigation was performed in two steps. In the first step we solved the system of equations (6) for a fixed instant of time $t_1 = \tau/T_1$ to which the dimensionless instant frequency $\Omega = \Omega_1/\Omega_0$ corresponds. The results of calculations performed for characteristic sections in the beginning and end of the stage were stored. Apart from the amplitudes $A_{jn}(x, y, \Omega) = A_{jn}(\boldsymbol{r}_\perp, \Omega)$ of the waves, their dimensionless 'angular' spectrum was also calculated:

$$B_{jn}(q_x, q_y, \Omega) = B_{jn}(\boldsymbol{q}, \Omega) = \iint A_{jn}(\boldsymbol{r}_\perp, \Omega)\exp(\mathrm{i}\boldsymbol{q}\boldsymbol{r}_\perp)\mathrm{d}\boldsymbol{r}_\perp.$$

The function

$$B_n(q_x, q_y, \Omega) = \left(1 + \frac{\omega_1}{\omega_1^{(0)}}\right)B_{1n}(q_x, q_y, \Omega)$$

determines the field in the focal region of a lens (or a focusing mirror) with the focal distance F:

$$E_{1n}(x_f, y_f, \Omega) = \mathrm{i}\,\frac{k_1^{(0)} a_{pn}}{2\pi F}\left(\frac{I_p \lambda_1^{(0)}}{\lambda_3^{(0)}}\right)^{1/2} B_n(q_x, q_y, \Omega). \qquad (9)$$

Here, a_{pn} is the pump-beam radius in the nth stage; $q_x = q_x^{(0)}(1 + \Omega)$; $q_y = q_y^{(0)}(1 + \Omega)$; $q_x^{(0)} = \theta_x/\theta_{dn}$; $q_y^{(0)} = \theta_y/\theta_{dn}$; $\theta_{dn} = 1/(k_1^{(0)} a_{pn})$; $\theta_x = x/F$; and $\theta_y = y/F$.

In the second step the development of the process in time was investigated. We calculated the Fourier transform for each function $A_{jn}(x, y, \Omega)$ or $B_n(q_x, q_y, \Omega)$

$$\bar{A}_{jn}(x, y, t_0) = \int A_{jn}(x, y, \Omega)\exp[\mathrm{i}\Phi_{A\mathrm{cor}}(\Omega)]\exp(\mathrm{i}t_0\Omega)\mathrm{d}\Omega,$$

$$\bar{B}_n(q_x, q_y, t_0) = \int B_n(q_x, q_y, \Omega)\exp[\mathrm{i}\Phi_{B\mathrm{cor}}(\Omega)]\exp(\mathrm{i}t_0\Omega)\mathrm{d}\Omega,$$

thereby determining the dependence of the amplitudes $\bar{A}_{jn}(x, y, t_0)$ and $\bar{B}_{jn}(q_x, q_y, \Omega)$ of a compressed pulse on time $t_0 = t/\tau_0$. The parameters of this pulse were determined by assuming that the compressor introduces frequency-dependent phase incursions $\Phi_{A\mathrm{cor}}(\Omega)$ and $\Phi_{B\mathrm{cor}}(\Omega)$ compensating the phase incursion $\Phi_{str}(\Omega)$ in the stretcher and the linear phase incursion in the amplifier. The frequency dependence of the nonlinear phase incursion was determined in calculations and presented as the sum of the approximating polynomial (up to the fifth degree) and the residual phase. The characteristics of the compressed pulse could be calculated when this phase incursion was completely compensated and also when it was completely or partially compensated by the approximating polynomial.

Consider additional assumptions which are used in simulations of the interaction of frequency-modulated beams.

In the general case the wave packet of the pump has the comet-shaped profile due to saturation. In the case of moderate saturation, the pulse shape at the central part is close to Gaussian (see, for example, [41]), while the cross-sectional intensity distribution weakly differs from the radiation intensity distribution at the amplifier input. Therefore, the expression for the amplitude $A_{pn}(\boldsymbol{r}_\perp, t)$ at the input surface of the nonlinear element of the nth stage with the independent pump can be written in the form

$$A_{pn}(x, y, t) = \left(\frac{I_{pn}}{I_p}\right)^{1/2}\exp\left(-\frac{t^2}{2T_{pn}^2}\right)\times$$

$$\times \cos^2\left[\frac{\pi}{2}\left(r^2\right)^{m_n}\right] \text{ при } r^2 = x^2 + y^2 < 1, \qquad (10)$$

$$A_{pn}(x, y, t) = 0 \text{ при } r^2 > 1.$$

Here, I_{pn} is the pump-wave intensity at the input of the nth stage; I_p is the pump-wave intensity at the input of the first stage of a preamplifier; and m_n is the 'super-Gaussian' exponent characterising the shape of the beam cross section. The coordinates x and y are normalised to the pump-beam radius of the corresponding channel ($x = x/a_{pn}^{(x)}$, $y = y/a_{pn}^{(y)}$). The possibility is provided for introducing into the right-hand side of (9) the factors simulating the dependences of the amplitude and phase modulation of pump beams on the transverse coordinates according to the harmonic law the quadratic dependence of the phase on r. The signal radiation pulse at the amplifier input is assumed Gaussian. Note that, to determine its energy, it is necessary to introduce the correction factor equal to $\sim 1.2 - 1.5$ because the amplitude of real pump radiation differs from amplitude (10).

The interacting wave beams from the output of a previous stage are projected to the input of a next stage with the specified signs and values of shifts, magnification, and the transfer coefficient. It is also possible to introduce filters of the angular spectrum of the beam transmitted in projection devices.

We simulated processes in a multistage system with the amplification of a short pulse in the first stage of the preamplifier and suppression of luminescence at its output. The scheme of the amplifier is shown in Fig. 3. Such an amplifier is excited by femtosecond pulses of the idler [25, 26] or signal wave with energy $W_0 = 1$ nJ. The exciting pulse first propagates through preliminary stretcher (*1*), in which it is stretched up to $T_1^{(0)} \approx 10 - 40$ ps. This is necessary to provide linear amplification ($10^3 - 10^4$) in the first stage. In addition, the amplification of such a stretched pulse weakly depends on the frequency 'slipping' effect. Note that the linear amplification of a short pulse located at the centre of a long pump pulse is described almost exactly by equations in the quasi-static approximation.

After the propagation of a pulse exciting the first stage through the pulse shaping system and amplification of this pulse up to a few microjoules in this stage, the signal radiation pulse was compressed down to its initial duration in compressor (*3*) and then passed through nonlinear filter (*4*), which did not transmit luminescence from the first stage. As such a filter it is convenient to use a device based on nonlinear birefringence like that studied in [35]. We assumed in calculations that the nonlinear filter is inertialless and its saturation intensity is so low that changes in the shape and phase of the signal spectrum can be neglected. It was also assumed that the signal was attenuated after filtering by an order of magnitude.

After the suppression of luminescence, the signal pulse propagates through main stretcher (*5*) and then is amplified in the second stage. We assumed in calculations that optical systems transfer to the input of this stage the inverted (with respect to the coordinate origin) images of the pump and signal radiation emerging from the first stage, not changing angles between these radiation beams and the optical axis of the nonlinear element (or change the signs of the angles but do not invert images). In this scheme of connection of stages, the amplification cone of the second stage is inverted with respect to the luminescence cone of the first stage, and effects related to the relative pulling down of the beams are somewhat compensated. When the first stage was excited by the idler wave with the beam radius $a_{20} = 0.12$ cm, the beam radius of signal radiation transferred to the second stage increased by a factor of five.

The length of nonlinear DKDP elements can achieve 12 cm. Therefore, when the peak intensity of pump radiation at the input to a preamplifier achieves $I_p \approx 1$ GW cm^{-2}, its efficient conversion to signal radiation can occur in the second stage. This case was considered in the simulation of a scheme with a two-stage preamplifier (scheme 1). When the preamplifier operates at lower radiation intensities $I_p \leqslant 0.8$ GW cm^{-2}, the third preamplification stage is required. The two variants of connection of the third stage are possible. In the first case, the third stage is connected to the second stage by using coherent excitation when all the three interacting waves propagate through a rather narrow gap to a nonlinear element of the third stage not changing the shape of the beams and phase matching (scheme 2). In the second case (scheme 3a), the connection between the second and third stages is similar to that between the first and second stages in the scheme with the inversion of the phase-matching cone. After preliminary amplification, the signal-beam diameter increases by a factor of 12 and the beam is amplified in the first stage and then, after its diameter is further increased twice, the beam is amplified in the second final stage. Table 1 presents the parameters of scheme 3 with the reduced pump intensity and energy (scheme 3b) and the narrowed transmission band of a stretcher (scheme 3c).

The operation of the amplifier was simulated with pumping parameters chosen close to the achieved [26–28] or expected parameters (see Table 1). The radii $\tilde{a}_{pn}$ of pump beams at the input of final stages and lengths of their nonlinear elements in all calculations were fixed ($\tilde{a}_{p1} = 6$ cm, $\tilde{a}_{p2} = 12$ cm, $\tilde{d}_1 = 8$ cm, $\tilde{d}_2 = 3.5$ cm). We also fixed pump-pulse durations in all stages ($T_p = \tilde{T}_{p1} = 1$ ns, $\tilde{T}_{p2} = 1.2$ ns) and the pump intensity at the input of the final stage $\tilde{I}_{p2} = 1.4$ GW cm^{-2}. It was also assumed that the radiation intensity distribution in the pump beam in the preliminary amplifier is super-Gaussian with $m_n = 4$. Calculations in final stages were performed both for $m_n = 2$ (the pump-pulse energy in the final stage was $\tilde{W}_{p2} = 795$ J) and for $m_n = 4$ ($\tilde{W}_{p2} = 1024$ J). It was found that, when the value

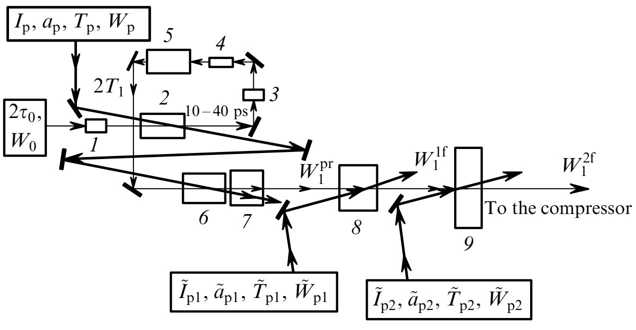

Figure 3. Scheme of the parametric multistage amplifier: (*1*, *5*) stretchers; (*3*) compressor; (*4*) nonlinear filter; (*2*, *6*, *7*) preamplifier stages; (*8*, *9*) final amplifier stages; the thin straight lines parallel to the system axis are the signal wave; the thick straight lines are the pump wave.

Table 1. Parameters of the preamplifier.

Scheme number	Preamplifier scheme	I_p/ GW cm^{-2}	W_p/J	a_{p0}/cm	a_{10}/cm	d_1/cm	d_2/cm	d_3/cm	$\tilde{I}_{p1}$/ GW cm^{-2}	$\tilde{W}_{p1}$/J
1	Two-stage scheme	1.0	1.09	0.5	0.4	11	10	–	1.2	145.5
2	Scheme with coherent excitation of the third stage	0.8	0.87	0.5	0.5	12	8.0	7.0	1.0	121.3
3a	Scheme with the inversion of the phase-matching cone of the third stage ($\Omega_{str} = \Delta\Omega_{max}$)	0.8	1.25	0.6	0.5	12	9.6	7.0	1.0	121.3
3b	Scheme with the inversion of the phase-matching cone of the third stage ($\Omega_{str} = \Delta\Omega_{max}$)	0.7	1.1	0.6	0.5	12	9.6	7.0	1.0	121.3
3c	Scheme with the inversion of the phase-matching cone of the third stage ($\Omega_{str} = 0.8\Delta\Omega_{max}$)	0.8	0.87	0.5	0.5	12	9.6	7.0	1.0	121.3

Note: a_{p0} and a_{10} are the pump and signal beam radii, respectively; d_1, d_2, and d_3 are the lengths of DKDP elements in the preamplifier; I_p and $\tilde{I}_{p1}$ are pump intensities in the first stages of the preamplifier and final amplifier, respectively; W_p and $\tilde{W}_{p1}$ are the corresponding pump energies.

of m_n was changed, all other factors being the same, the energy and power of the amplified pulse changed proportionally to the filling factor K_{m_n} of the pump beam with an accuracy of a few percent ($K_{m_n} = 0.59$ for $m_n = 2$ and 0.76 for $m_n = 4$); the pulse shape and duration almost did not change. Tables 1 and 2 present the values of parameters for $m_n = 2$. Calculations were performed for two transmission bandwidths of the stretcher $\Omega_{str} = \Delta\Omega_{max}$ and $0.8\Delta\Omega_{max}$, where $\Delta\Omega_{max}$ is the limiting width of the gain band (estimated below).

The beam radius of an idler wave exciting the amplifier was set equal to $a_{20} \approx 0.12$ cm, which is approximately five times smaller than the pump beam radius a_p. This is necessary to reduce the influence of the phase inhomogeneity of the pump beam. When the amplification band of a signal is close to its limiting value, a small radius of the exciting beam leads to a noticeable dependence of the signal intensity amplified in the first stage on the instant frequency of the radiation pattern. The angular-frequency characteristic for $q_y = 0$ for this case is presented in Fig. 4a. The frequency dependence of the signal propagation direction can be almost completely compensated by the proper choice

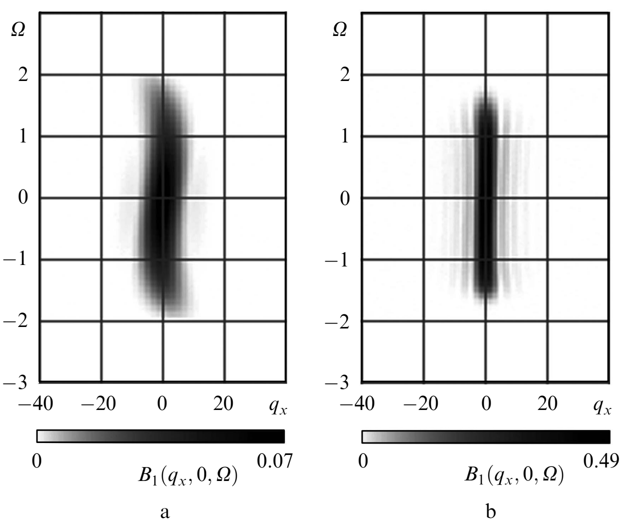

Figure 4. Dependences of the signal wave intensity $B_1(q_x, 0, \Omega)$ on frequency Ω and wave number q_x at the outputs of the first (a) and final stages (b).

of parameters of the subsequent stages of the preamplifier, as illustrated in Fig. 4b. We will not discuss here the details of such compensation. Note only that scheme 3 of a preamplifier excited by an idler wave allows the generation of compressed pulses with parameters close to the parameters of pulses excited directly by signal radiation, which are considered below.

When the amplifier is excited by signal radiation, it is expedient to make the beam radius a_1 equal to the radius of the pump beam of the first stage. Because the angle $\beta_{p2} = \tilde{\beta}_p - \tilde{\beta}_2$ between the group velocities of the idler and pump waves is small compared to the angle $\tilde{\beta}_2$ between the group velocities of amplified waves ($|\beta_{p2}| \approx (0.004 \div 0.02)\Omega_1$, $|\tilde{\beta}_2| \approx 0.041$), the amplification of such a beam is weakly sensitive to the phase inhomogeneities of the pump beam with the transverse scale Δ_Φ exceeding the relative displacements $|\beta_{p2}|d_n$ of the pump and idler wave beams over the length of a nonlinear element, and also to small-scale inhomogeneities of the pump-beam intensity in the zx plane (of the scale $\Delta_1 < |\tilde{\beta}_p|d_n \approx a_p$). The inhomogeneities of the pump intensity in the zy plane, even if they are weak (no more than $0.1I_p$), can produce the noticeable modulation of the signal intensity (a few tens of percent). Calculation show that such a modulation weakly changes the gain averaged over the cross section (in the nonlinear regime – the pump conversion coefficient). Spatial filters mounted behind each stage of the preamplifier reduce down to ~ 1 % the influence of this modulation on the parameters of a signal amplified in final stages.

When a broad beam is amplified, a change in its propagation direction with deviation of the frequency from the exact phase-matching frequency becomes almost unnoticeable. We consider in more detail the parameters of amplifiers excited in this way.

The parameters of final stages of the preamplifier (second or second and third) were selected in calculations to provide the moderate 'supersaturation' operation regime of the output stage, when the maximum of the conversion coefficient is achieved inside a nonlinear element and then this coefficient decreases approximately by half. The lengths of nonlinear elements in two final stages and power transfer coefficients between the stages were selected so that these stages operated in the regime close to saturation.

We also assumed in calculations that the spectral width $2\Omega_0 = 2/\tau_0$ of the amplified signal at the amplifier input was smaller by half than the transmission bandwidth Ω_{str} of the stretcher, while the duration T_{str} of the amplified pulse was equal to the doubled duration of the stretched input pulse. In this case, the intensity of the spectral components of this pulse at the wings of the transmission band was e^{-4} of the maximum intensity.

The main goal of calculations presented below was to elucidate the possibility of increasing the energy and improving parameters (power, the leading edge steepness, and contrast achieved at the leading edge) of the compressed pulse by varying the amplified pulse duration T_{str} when the transmission bandwidth Ω_{str} of the system was close to the limiting gain bandwidth $\Delta\Omega_{max}$.

The width $\Delta\Omega_{max}$ depends on the pump intensity and is determined by the angle $\Psi_p^{(0)} \approx 0.023$ rad between the signal and pump beams in amplifier stages. This value of the angle was chosen so that for $I_{pn} \sim 1$ GW cm^{-2} the condition $[\Delta K/(2\gamma_0)]^2 \ll 1$, $\gamma_0 \approx 0.6$ cm^{-1}] of the weak influence of the wave detuning on the amplification process was violated only at the wings of the transmission band (the wave detuning at the central region of this band did not exceed 0.02 cm^{-1}, while at the wings it did not exceed 0.1 cm^{-1}). It follows from analysis of the tuning parameters of a DKDP crystal that the limiting amplification bandwidth in the case of such adjustment is $\Delta\Omega_{max} = 0.47$ fs^{-1} (analysis was performed by using Sellmeyer relations presented in [42]; see also [26]). The dependence of the wave detuning on the frequency Ω_1 in this band was approximated by the third-degree polynomial $\Delta K = 3.54\Omega_1 + 2\Omega_1^2 - 122.4\Omega_1^3$.

Calculations performed in the one-dimensional approximation showed that in the case of the optimal adjustment (when $[\Delta K/(2\gamma_0)]^2 \ll 1$ in the transmission band), the energy of the amplified pulse and its dimensionless effective duration

$$\tau_{eff} = \int_{-\infty}^{\infty} |\bar{A}_1^f(0,0,t_0)|^2 dt_0 / \bar{A}_1^f(0,0,t_0)|^2$$

[$t_0 = t/\tau_0$ and $\bar{A}_1^f(0,0,t_0)$ is the function describing the field structure at the final stage output] after compression weakly depend on the spectral width of the pulse up to its limiting value $2\Omega_{0\,max} = \Delta\Omega_{max}/2$. This corresponds to $\tau_{0\,min} = 8.5$ fs. In this case, the pulse energy and τ_{eff} weakly change with changing the operation regime of the preamplifier: $\tau_{eff} \approx 1.95$ in the supersaturation regime, while in the saturation regime the effective pulse duration increases up to $\tau_{eff} \approx 2.1$ and the pulse energy decreases approximately by 10 %.

As Ω_0 is further increased (up to $\Omega_m = 0.14$ fs$^{-1} > \Omega_{0\,max}$), the requirement $[\Delta K/(2\gamma_0)]^2 \ll 1$ within the entire transmission band $\Omega_{str} = 4\Omega_m$ of the system cannot be fulfilled because $[\Delta K/(2\gamma_0)]^2 \approx 1$ at some points. This leads to the reduction of the pump conversion efficiency and the energy and power of the amplified pulse. These conclusions were confirmed and refined by calculations in the approximation of quasi-static amplification of frequency-modulated beams.

The dimensionless effective pulse duration τ_{eff}^f in these calculations was determined from the calculated time dependence of the amplitude $\bar{B}_1^f(0,0,t_0)$ at the centre of the focal spot of a compressed pulse

$$\tau_{eff}^f = \int_{-\infty}^{\infty} |\bar{B}_1^f(0,0,t_0)|^2 dt_0 / |\bar{B}_1^f(0,0,0)|^2 .$$

The dimensionless divergence of this radiation $\Delta\theta_1/\Delta\theta_{dpn} \approx 2.4$, where $\Delta\theta_{dpn} = 1/(k_1^{(0)} a_{pn})$, in all calculations is close to the divergence of a beam of radius close to the radius of the pump beam of the output stage and having the homogeneous intensity distribution.

Table 2 presents the output energies W_1^{pr}, W_1^{1f}, and W_1^{2f} of the first and second stages of the main amplifier, and the duration τ_{eff}^f and power P_1^f of the compressed pulse (by neglecting losses in the compressor) in the case of the complete compensation of the nonlinear phase incursion calculated for three schemes at some values of parameters I_p, a_p, T_{str}, and τ_0. Note that the compensation of this incursion accurate to the approximating polynomials of fifth and third degrees noticeably, approximately by 5 %, leads to the increase in τ_{eff}^f only in the scheme with coherent excitation of the third stage of the preamplifier. The pulse full width at half-maximum $\tau_{0.5}^f$ is smaller than τ_{eff}^f approximately by 10 %.

One can see from Table 2 that the signal pulse energy at the final stage output for all three amplifier schemes increases approximately by 30 % with increasing T_{str} from 1.2 to 2.4 ns. The effective pulse duration increases somewhat slower. As a result, its peak intensity almost does not change. As T_{str} is further increased, the pulse power begins to decrease because τ_{eff}^f noticeably increases (from 2 to 2.35 for $T_{str} = 2.4$ ns) despite a small increase in energy.

The shape and duration of the fronts of the compressed pulse depend stronger on the preamplifier scheme and the amplified pulse duration.

In the limiting case $\Omega_{str} \approx \Delta\Omega_{max}$, the compressed pulse structure begins to depend considerably on the nonlinear

Table 2. Output parameters of amplifiers.

Scheme number	I_p/GW cm^{-2}	a_{p0}/cm	T_{str}/ns	τ_0/fs	W_1^{pr}/J	W_1^{1f}/J	W_1^{2f}/J	τ_{eff}^f	P_1^f/PW
1	1.0	0.5	1.5	8.5	0.16	37	234	1.8	15.3
1	1.0	0.5	2.0	8.5	0.18	42	272	2.0	16.0
2	0.8	0.5	1.5	8.5	0.10	29	246	1.9	15.2
2	0.8	0.5	2.0	8.5	0.13	31	270	2.1	15.1
3a	0.8	0.5	1.2	8.5	0.125	27	219	1.63	15.8
3a	0.8	0.5	2.0	8.5	0.154	33	280	2.0	16.4
3a	0.8	0.5	2.4	8.5	0.153	33	280	2.35	14.0
3a	0.8	0.6	1.5	8.5	0.2	35	260	1.8	17.0
3a	0.8	0.6	2.0	8.5	0.26	37	290	2.0	17.1
3b	0.7	0.6	2.0	8.5	0.14	32	262	2.15	14.3
3c	0.8	0.6	1.2	10.6	0.18	29	238	1.57	14.3
3c	0.8	0.6	2.0	10.6	0.22	37	287	1.97	13.7

phase incursion $\Delta\Phi_{\rm nl}(\Omega)$ of the amplified wave (Fig. 5). By adjusting the stretcher-compressor system, this phase incursion can be compensated up to the third or fifth order of its expansion in powers of frequency Ω. After such correction for $\Omega_{\rm str} < \Delta\Omega_{\max}$, the effective pulse duration in schemes studied becomes almost equal to the transform-limited pulse duration. However, for $\Omega_{\rm str} = \Delta\Omega_{\max}$ in scheme 2, the noticeable phase incursion $\Delta\Phi_{\rm res}(\Omega)$ remains (Fig. 5).

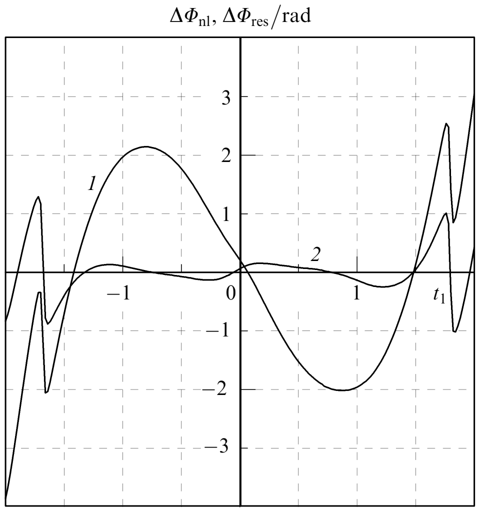

Figure 5. Nonlinear phase incursion $\Delta\Phi_{\rm nl}$ (*1*) of the signal wave in amplifier scheme 2 and the residual phase incursion $\Delta\Phi_{\rm res}$ (*2*) for $T_{\rm str} =$ 1.5 ns.

The shape and duration of the pulse leading front for amplifier schemes 1 and 3 differ insignificantly. The residual phase incursion in these schemes did not exceed 0.2 rad, and after the compensation of the nonlinear phase incursion up to the third or fifth order, the pulse almost completely coincides with the transform-limited pulse. The pulse fronts exhibit weak oscillations with period of $\sim \tau_0$. The averaged amplitude decreases exponentially down to some level, which we will call the pulse contrast. The steepness of the exponential part noticeably depends on the stretched pulse duration and increases approximately twice with increasing $T_{\rm str}$ from 1.2 to 2.4 ns (Fig. 6).

It is important that, when the pump pulse energy of the intermediate amplifier is decreased by 10 %, the frequency dependence of the nonlinear phase incursion changes insignificantly, so that the shape of pulse fronts remains almost invariable and the effective pulse duration increases due to a small change in the spectral width of the pulse (less than by 10 %) (Table 2).

In scheme 2 with coherent excitation of the third stage of the preamplifier, the leading front of the pulse noticeably differs from exponential and its duration is approximately 1.5 times longer than that in schemes 1 and 3, even when the phase incursion is completely compensated. In addition, the residual phase incursion in this case is larger than that for schemes 1 and 3 (Fig. 5) and noticeably affects the shape of pulse fronts (Fig. 7). This is explained by the fact that upon coherent excitation of the third stage of the preamplifier, the nonlinear elements of the second and third stages are in fact combined. As a result, the amplification process is subjected to a stronger influence of the asymmetry of the dependence of the effective interaction coefficient $\gamma(\Omega_1) = [\gamma_1(\omega_1)\times$

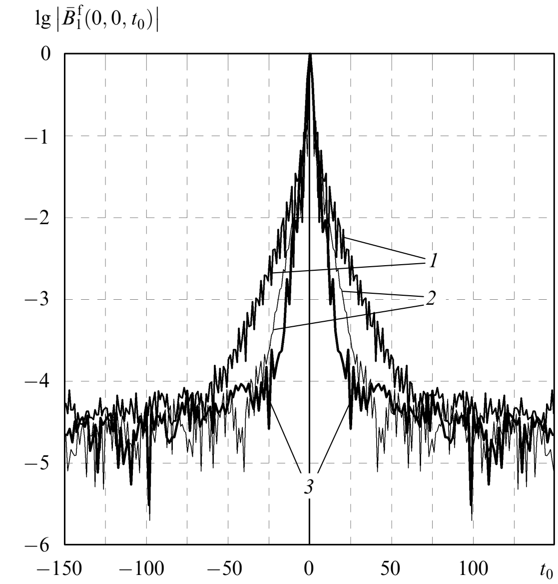

Figure 6. Time dependences of the amplitude $|\bar{B}_1^{\rm f}(0,0,t_0)|$ at the centre of the focal spot of a compressed radiation pulse for preamplifier scheme 3a for $T_{\rm str} = 1.2$ (*1*), 2 (*2*), and 2.4 ns (*3*).

$\gamma_2(\omega_2)]^{1/2}$ on the signal frequency and also of different directions of the group velocities of the waves because the relative displacement $(d_2 + d_3)|\beta_2|$ of their beams exceeds the pump beam radius almost by a factor of 1.5. When the signal width is close to the limiting value, this leads to a strong asymmetry of the dependence of the output power of the intermediate amplifier on the local frequency, which is preserved in final stages (Fig. 8), and also complicates the dependence of the nonlinear phase incursion on this frequency (Fig. 5).

The pulse contrast is determined by the amplitude of spectral components at the wings of the stretcher transmission band, which was assumed sharply restricted. For

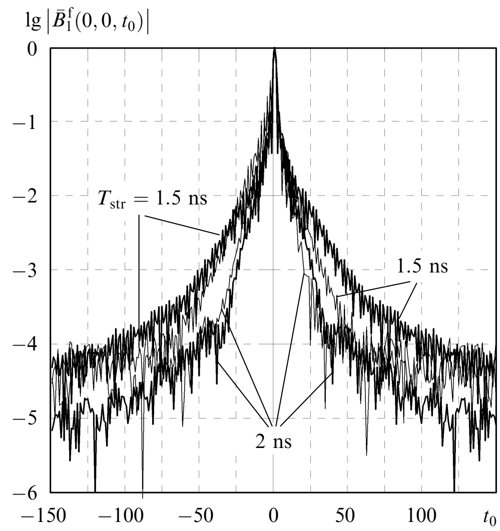

Figure 7. Dependences of the amplitude $|\bar{B}_1^{\rm f}(0,0,t_0)|$ at the centre of the focal spot of a compressed radiation pulse for amplifier scheme 2 in the case of the complete compensation of the nonlinear phase incursion (thick curves) and upon the correction of the nonlinear phase incursion up to the third order (thin curves).

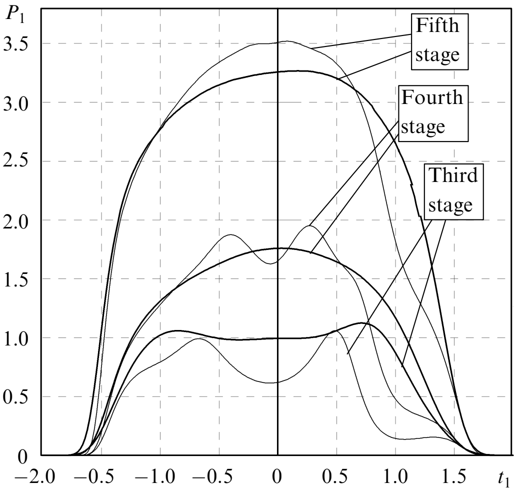

Figure 8. Time dependences of the output powers $P_1(t_1) = \iint |A_1(x, y, t_1)|^2 dxdy$ of the third, fourth, and fifth stages for amplifier scheme 2 (thin curves) and scheme 3a (thick curves).

$\Omega_{str} = \Delta\Omega_{max}$, the wave detuning ΔK at the wings of the transmission band is comparable with the interaction coefficient γ_0, and the gain in each stage decreases compared to the gain of central components by three–four orders of magnitude. Therefore, in this case the pulse contrast is high ($\sim 10^9 - 10^{10}$) in the entire range of the amplified pulse duration T_{str} (1.2 ns $\leqslant T_{str} \leqslant$ 2.4 ns). The decrease in the transmission bandwidth Ω_{str} down to $0.8\Delta\Omega_{max}$ (upon the corresponding decease in the spectral width of the signal) without changing the angle Ψ_p leads to a strong dependence of the pulse contrast on T_{str} (Fig. 9) because for $T_{str} = 1.2$ ns the gains at the wings of the spectrum and at its central part are close, while for $T_{str} = 2$ ns the gain at the wings considerably decreases due to the noticeable decrease in the pump intensity in this region. In the case of a constant duration T_{str}, the pulse contrast can be increased in the case under study by narrowing down the amplification band by changing the angle Ψ_p.

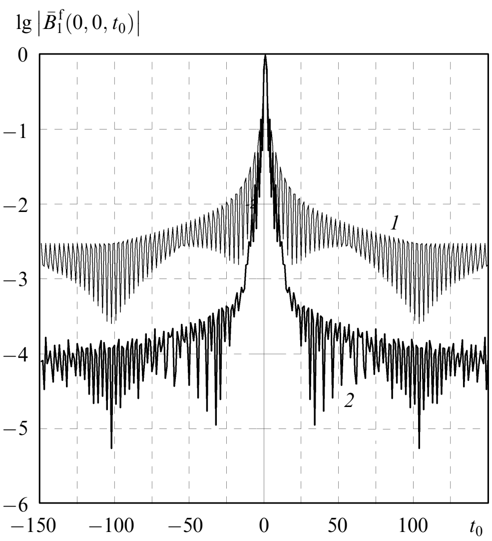

Figure 9. Dependences of the amplitude $|\bar{B}_1^f(0, 0, t_0)|$ at the centre of the focal spot of a compressed radiation pulse for amplifier scheme 3 for $\Omega_{str} = 0.8\Delta\Omega_{max}$, $T_{str} = 1.2$ (*1*) and 2 ns (*2*).

4. Conclusions

The main results obtained in the paper are:

(i) We have obtained relations allowing us to determine the applicability of the quasi-static approximation for the description of parametric amplification of frequency-modulated light beams for the gain bandwidth close to the limiting value. For BBO and DKDP crystals, the quasi-static approximation is applicable when the duration of pulses with the limiting spectral width increases up to several picoseconds and above.

(ii) By using nanosecond pump pulses at $\lambda_p \approx 500$ nm, it is possible to create a DKDP crystal amplifier with suppressed luminescence for pulses of duration down to 17 fs and power at the compressor output ~ 10 PW.

(iii) The steepness of the leading edge of a compressed pulse and its contrast increase with increasing the amplified pulse duration approximately up to the duration of pump pulses of final stages.

Acknowledgements. This work was supported by the Program of the President of the Russian Federation for the State Support of Leading Scientific Schools of the Russian Federation (Grant Nos NSh-1652.2003.2 and NSh-4690.2006.2) and the Program 'Femtosecond Optics and New Optical Materials' of the Presidium of the Russian Academy of Sciences and the Program 'Nonlinear Optics of Unique Laser Systems' of the Department of Physical Sciences of RAS.

References

1. Piskarskas A., Stabinis A., Yankauskas A. *Usp. Fiz. Nauk*, **150**, 127 (1986).
2. Dubietis A., Jonusauskas G., Piskarskas A. *Opt. Commun.*, **88**, 437 (1992).
3. Shirakawa A., Kobayashi T. *Appl. Phys. Lett.*, **72**, 147 (1998).
4. Cerullo G., Nisoli M., De Silvestri S. *Opt. Lett.*, **23**, 1283 (1998).
5. Shirakawa A., Sakane I., Kobayashi T. *Opt. Lett.*, **23**, 1292 (1998).
6. Shirakawa A., Sakane I., Takasaka M., Kobayashi T. *Appl. Phys. Lett.*, **74**, 2268 (1999).
7. Baltuška A., Fuji T., Kobayashi T. *Opt. Lett.*, **27**, 306 (2002).
8. Zinkstok R.Th., Witte S., Hogervorst W., Eikema K.S.E. *Opt. Lett.*, **30**, 78 (2005).
9. Ishii N., Turi L., Yakovlev V.S., Fuji T., Krausz F., Baltuška A., Butkus R., Veitas G., Smilgevičius V., Danielius R., Piskarskas A. *Opt. Lett.*, **30**, 567 (2005).
10. Tavella F., Schmid K., Ishii N., Marcinkevičius A., Veisz L., Krausz F. *Appl. Phys. B*, **81**, 753 (2005).
11. Tavella F., Marcinkevičius A., Krausz F. *New J. Phys.*, **8**, 219 (2006).
12. Tavella F., Marcinkevičius A., Krausz F. *Opt. Express*, **14**, 12822 (2006).
13. Ishii N., Teisset C.Y., Fuji T., Köhler S., Schmid K., Veisz L., Baltuška A., Krausz F. *IEEE J. Sel. Top. Quantum Electron.*, **12**, 173 (2006).
14. Witte S., Zinkstok R.Th., Wolff A.L., Hogervorst W., Ubachs W., Eikema K.S.E. *Opt. Express*, **14**, 8168 (2006).
15. Tavella F., Nomura Y., Veisz L., Pervak V., Marcinkevičius A., Krausz F. *Opt. Lett.*, **32**, 2227 (2007).
16. Renault A., Kandula D.Z., Witte S., Wolf A.L., Zinkstok R.Th., Hogervorst W., Eikema K.S.E. *Opt. Lett.*, **32**, 2363 (2007).
17. Adachi S., Ishii H., Kanai T., Ishii N., Kosuge A., Watanabe S. *Opt. Lett.*, **32**, 2487 (2007).
18. Kiriyama H., Mori M., Nakai Y., Ymamoto Y., Tonoue M., Akutsu A., Shimomura T., Kondo S., Kanazawa S., Daido H., Kimura T., Miyanaga N. *Opt. Lett.*, **32**, 2315 (2007).

19. Dorrer C., Begishev I.A., Okishev A.V., Zuegel J.D. *Opt. Lett.*, **32**, 2143 (2007).
20. Ross I.N., Matousek P., Towrie M., Langley A.J., Collier J.L. *Opt. Commun.*, **144**, 125 (1997).
21. Matousek P., Rus B., Ross I.N. *IEEE J. Quantum Electron.*, **36** (2), 158 (2000).
22. Ross I.N., Matousek P., New G.H.C., Osvay K. *J. Opt. Soc. Am. B*, **19**, 2945 (2002).
23. Xiaodong Yang, Zhi-zhan Xu, Yu-xin Leng, Hai-he Lu, Zheng-guan Zhang, Ru-xin Li, Wen-qi Zhang, Ding-jun Yin, Bing Tang. *Opt. Lett.*, **27**, 1135 (2002).
24. Chekhlov O.V., Collier J.L., Ross I.M., Bates P.K., Notley M., Hernandez-Gomez C., Shaikh W., Danson C.N., Neely D., Matousek P., Hancock S. *Opt. Lett.*, **31**, 3665 (2006).
25. Freidman G., Andreev N., Ginzburg V., Katin E., Khazanov E., Lozhkarev V., Palashov O., Sergeev A., Yakovlev I. *Proc. SPIE Int. Soc. Opt. Eng.*, **4630**, 135 (2002).
26. Andreev N.F., Bespalov V.I., Bredikhin V.I., Garanin S.V., Ginzburg V.N., Dvorkin K.L., Katin E.V., Korytin A.I., Lozhkarev V.V., Palashov O.V., Rukavishnikov N.N., Sergeev A.M., Sukharev S.A., Freidman G.I., Khazanov E.A., Yakovlev I.V. *Pis'ma Zh. Eksp. Teor. Fiz.*, **79**, 178 (2004).
27. Lozhkarev V.V., Garanin S.V., Gerke R.R., Ginzburg V.N., Katin E.V., Luchinin G.A., Mal'shakov A.N., Mart'yanov M.A., Palashov O.V., Poteomkin A.K., Rukavishnikov N.N., Sergeev A.M., Sukharev S.A., Freidman G.I., Khazanov E.A., Charukhchev A.V., Shaikin A.A., Yakovlev I.V. *Pis'ma Zh. Eksp. Teor. Fiz.*, **82**, 196 (2005).
28. Lozhkarev V.V., Freidman G.I., Ginzburg V.N., Katin E.V., Khazanov E.A., Kirsanov A.V., Luchinin G.A., Mal'shakov A.N., Martyanov M.A., Palashov O.V., Poteomkin A.K., Sergeev A.M., Shaykin A.A., Yakovlev I.V., Garanin S.G., Sukharev S.A., Rukavishnikov N.N., Charukhchev A.V., Gerke R.R., Yashin V.E. *Opt. Express*, **14**, 446 (2006).
29. Lozhkarev V.V., Freidman G.I., Ginzburg V.N., Katin E.V., Khazanov E.A., Kirsanov A.V., Luchinin G.A., Mal'shakov A.N., Martyanov M.A., Palashov O.V., Poteomkin A.K., Sergeev A.M., Shaykin A.A., Yakovlev I.V. *Laser Phys. Lett.*, **4**, 421 (2007).
30. http://www.extreme-light-infrastructure.eu/pictures/ELI-scientific-case-id17.pdf.
31. Belyaev Yu.N., Kiselev A.M., Freidman G.I. *Pis'ma Zh. Eksp. Teor. Fiz.*, **9**, 441 (1969).
32. Di Trapani P., Andreoni A., Solcia C., Foggi P., Danielius R., Dubietis A., Piskarskas A. *J. Opt. Soc. Am.*, **12**, 2237 (1995).
33. Itatani J., Faure J., Nantel M., Mourou G., Watanabe S. *Opt. Commun.*, **148**, 70 (1998).
34. Hong K.-H., Hou B., Nees J.A., Power E., Mourou G.A. *Appl. Phys. B*, **81**, 447 (2005).
35. Cotel A., Jullien A., Forget N., Albert O., Cheriaux G., Le Blanc C. *Appl. Phys. B*, **83**, 7 (2006).
36. Vlasov S.N., Talanov V.I. *Samofokusirovka voln* (Self-focusing of Waves) (Nizhnii Novgorod, Institute of Applied Physics, RAS, 1997).
37. Bondarenko N.G., Eremina I.V., Makarov A. *Abstracts of Papers, V All-Russian Conference on Laser Optics* (Leningrad, 1987) p. 256.
38. Danielius R., Piskarskas A., Di Trapani P., Andreoni A., Solcia C., Foggi P. *Opt. Lett.*, **21**, 973 (1996).
39. Sushchik M.M., Morozov S.F., Piskunova L.V., Freidman G.I. *Kvantovaya Elektron.*, **3**, 548 (1976) [*Sov. J. Quantum Electron.*, **6**, 293 (1976)].
40. Dmitriev V.G., Gurzadyan G.G., Nikogosyan D.N. *Handbook of Nonlinear Optical Crystals* (Berlin, Heidelberg, New York: Springer-Verlag, 1999).
41. Jovanovic I., Ebbers C.A., Comaskey B.J., Bonner R.A., Morse E.C. *Opt. Express*, **12**, 446 (2004).
42. Kirby K.W., De Shazer L.G. *J. Opt. Soc. Am. B*, **4**, 1072 (1987).